REPORT DOCUMENTATION PAGE

Form Approved
OMB No. 0704-0188

1. AGENCY USE ONLY *(Leave blank)*	2. REPORT DATE	3. REPORT TYPE AND DATES COVERED
	February 1999	Final Report 1 Sep 96 - 30 Nov 98

4. TITLE AND SUBTITLE
"Study of the Creep Resistance in Ti-62222S Alloy"

5. FUNDING NUMBERS
F49620-96-1-0448

6. AUTHOR(S)
Professor Jun-ichi Koike

7. PERFORMING ORGANIZATION NAME(S) AND ADDRESS(ES)
Tohoku University
Department of Materials Science
Dendai 980-8579, Japan

8. PERFORMING ORGANIZATION REPORT NUMBER
N/A

9. SPONSORING/MONITORING AGENCY NAME(S) AND ADDRESS(ES)
Asian Office of Aerospace Research and Development (AOARD)
Unit 45002
APO AP 96337-5002

10. SPONSORING/MONITORING AGENCY REPORT NUMBER
AOARD-96-07

11. SUPPLEMENTARY NOTES
N/A

12a. DISTRIBUTION AVAILABILITY STATEMENT
Approved for public release; distribution unlimited.

12b. DISTRIBUTION CODE
A

13. ABSTRACT *(Maximum 200 words)*

Primary creep behavior was studied in Ti-6Al-2Sn-2Zr-2Cr-2Mo-0.16Si (Ti-6-22-22S) alloy. Creep tests were performed at 480 degrees C under various stresses in the range of 150 to 500 MPa. The creep behavior was analyzed in terms of Larson-Miller time to reach 0.1% creep strain. The results were compared with those in other Ti alloys as well as in Ti-6-22-22S reported by others. It was found that the a+B processed Ti-6-22-22S showed better creep resistance than the B processed alloy. It was also found that the a+B processed alloy showed much better creep resistance than Ti-6A1-4V (Ti-64) and is in general agreement with that of Ti-6A1-2Sn-4Zr-6Mo (Ti-6246). Therefore, the Ti-6-22-22S alloy is an attractive alloy not only for room-temperature applications but also for long term load-carrying applications near 400 degrees C and lower. The alloy may replace the existing Ti-6246 alloy and can be used for turbine engine parts at intermediate temperatures in addition to conventional applications to air frame parts.

14. SUBJECT TERMS
Creep behavior, creep resistance, load-carrying, creep strain, processed alloy.

15. NUMBER OF PAGES
20

16. PRICE CODE

17. SECURITY CLASSIFICATION OF REPORT	18. SECURITY CLASSIFICATION OF THIS PAGE	19. SECURITY CLASSIFICATION OF ABSTRACT	20. LIMITATION OF ABSTRACT
UNCLASSIFIED	UNCLASSIFIED	UNCLASSIFIED	PB

30 Nov 98

Study of the Creep Resistance in Ti-62222S Alloy

(Grant No. F49620-96-1-0448)

Final Report

Prof. Jun-ichi Koike

Dept. of Materials Science, Tohoku University
Sendai 980-8579, Japan

Tel/Fax: (022) 217-7325
e-mail: koikej@material.tohoku.ac.jp

ABSTRACT

Primary creep behavior was studied in Ti-6Al-2Sn-2Zr-2Cr-2Mo-0.16Si (Ti-6-22-22S) alloy. Creep tests were performed at 480 °C under various stresses in the range of 150 to 500 MPa. The creep behavior was analyzed in terms of Larson-Miller time to reach 0.1% creep strain. The results were compared with those in other Ti alloys as well as in Ti-6-22-22S reported by others. It was found that the $\alpha+\beta$ processed Ti-6-22-22S showed better creep resistance than the β processed alloy. It was also found that the $\alpha+\beta$ processed alloy showed much better creep resistance than Ti-6Al-4V (Ti-64) and is in general agreement with that of Ti-6Al-2Sn-4Zr-6Mo (Ti-6246). Therefore, the Ti-6-22-22S alloy is an attractive alloy not only for room-temperature applications but also for long-term load-carrying applications near 400 °C and lower. The alloy may replace the existing Ti-6246 alloy and can be used for turbine engine parts at intermediate temperatures in addition to conventional applications to air frame parts.

ACKNOWLEGEMENTS

This work was supported by US AFOSR-AOARD Grant #F49620-96-1-0448. The author is grateful to Prof. D. Eylon of U. Dayton, Prof. G. Luetjering of Technische Universitat Hamburg-Harburg, and Dr. S. Fujishiro of AOARD for their suggestions and fruitful discussion. Special thanks to Mr. Tom Kim of AOARD for his encouragement and support throughout the project work.

TABLE OF CONTENTS

1.	Introduction	1
2.	Experimental Procedure	2
3.	Results and Discussion	4
4.	Conclusion	6
5.	Reference	7
6.	Figure Captions	8

1. INTRODUCTION

Ti-6-22-22S (Ti-6Al-2Sn-2Zr-2Cr-2Mo-[0.12~0.20]Si) was developed in 1970s by RMI company for deep hardenability, high strength, and high fracture resistance [1]. The alloy can provide better damage tolerance with respect to strength than the Ti-6Al-4V (Ti-64) alloy [2, 3]. However, the study of this alloy had advanced slowly because of the lack of application at the time. Recently, renewed interest has been revived for an application to aircraft parts [4, 5]. Ti-6-22-22S has been chosen for applications on the U. S. Airforce F-22 fighter aircraft. Further application is scheduled on the X-33 Demonstrator/Reusable Launch Vehicle and the Joint Strike Fighter. At the moment, a strong research effort is underway to optimize room-temperature strength and fracture resistance through the variation of chemistry and thermomechanical processing [2, 3].

The original alloy stemmed from a Ti-6Al-2Sn-4Zr-2Mo-Si (Ti-6242) alloy, one of the most creep resistant alloy, and contained 0.23 wt.% Si in order to improve mechanical strength at room temperature and elevated temperature. However, addition of 0.23 wt.% Si was found to cause inhomogeneity of the Si concentration in ingots. In order to further optimize the Si concentration, Wood et al. investigated the effects of the Si concentration on tensile properties and fracture toughness [6]. They found that the Si concentration can be lowered to 0.15 wt.% without causing noticeable changes in mechanical properties. Based on their work, the allowance of the Si concentration was recommended to be limited in the range of 0.12 to 0.20 wt.%. In this regard, the Si concentration of the present alloy was chosen to be 0.16 wt.%.

In order to optimize tensile properties, the alloy is generally processed and heat treated in the $\alpha+\beta$ phase region. The alloy is also processed in the β phase region and heat treated in the $\alpha+\beta$ phase region for the optimization of fracture toughness and fatigue crack growth resistance. While most research has been focused on mechanical properties at room temperature, little work has been performed to characterize creep properties of the alloy. When the room-temperature mechanical properties are under consideration, the Ti-6-22-2S alloy has been compared with the Ti-64 alloy. On the other hand, when the creep resistance is under consideration, The Ti-6-22-22S alloy should be compared with Ti-6242 (a high creep resistant

near-α alloy) or with Ti-6246 (a creep resistant α+β alloy).

Up to date, there have been two separate reports regarding creep resistance of the alloy. The reported results are summarized in Fig. 1 together with the results of three common Ti alloys containing α+β phase [7]. The figure indicates stress versus Larson-Miller parameter for 0.2% creep strain. Temperature (T) and time (t) in the Larson-Miller parameter are in the units of °C and hour, respectively. As shown in the figure, Bartlo et al. performed creep experiments in an α+β processed alloy under high stresses of larger than 600 MPa [8]. Their data indicate that the creep resistance of the Ti-6-22-22S is comparable to that of Ti-6246 (Ti-6Al-2Sn-4Zr-6Mo in wt%). On the other hand, Kuhlman performed creep experiments in an β processed alloy under low stresses below 450 MPa [3]. His results indicate that the creep resistance of the Ti-6-22-22S alloy is much weaker than expected from the earlier report for higher stresses by Bartlo et al. and shows a strong stress dependence. This figure indicates that a better creep resistance can be obtained by processing in the α+β phase region. However, the creep data of the α+β processed alloy is so much limited that creep resistance cannot be estimated under practical application conditions.

The purpose of this paper is to characterize the primary creep behavior at 480 °C in a wide range of stress (150 to 500 MPa) in the α+β processed Ti-6-22-22S. The obtained results are compared with the previously reported results in other Ti alloys.

2. EXPERIMENTAL PROCEDURE

The alloy Ti-6-22-22S was manufactured and provided by J. R. Wood of RMI company. The alloy composition is given in Table 1. The β transus temperature of the alloy was between 960 and 970 °C [6]. The alloy was hot worked in the α+β phase region to an approximate size of 15x25x38 mm^3. The rods were then subjected to triplex heat treatment: solution treatment in the β phase region at 1004 °C (1840 °F) for 1 hour → fan cooling → solution treatment in the α+β phase region at 927 °C (1700 °F) for 1 hour → fan cooling → aging at 538 °C (1000 °F)

for 8 hours → air cooling to room temperature.

Table 1 Chemical composition of Ti-6-22-22S alloy (in wt.%)

Al	Sn	Zr	Cr	Mo	Si	Fe	O	N	H	Ti
5.44	1.99	1.99	2.06	2.16	0.16	0.09	0.11	0.006	62 *	bal.

* ppm

Fig. 2 (a) shows a typical microstructure observed by an optical microscope after triplex heat treatment. There is no difference in the microstructure between the length and the transverse directions of the provided rods, indicating the isotropic microstructure. The microstructure of the alloy consists of a primary α phase and a transformed β phase in a coarse lamellae shape. The α phase is also observed along the boundaries of the former β grains. Fig. 2 (b) shows a bright-field image of the same sample observed by a transmission electron microscope (TEM). The thickness of the primary α lamellae is approximately 1 μm. An acicular α phase is seen in the transformed β phase. With this structure, dislocation-glide motion is confined in the primary α lamellae and a substantial improvement of tensile strength and fatigue resistance is realized [9].

A standard-size tensile test samples were prepared by electrodischarge machining. The shape and size of the sample are given in Fig. 3. The length direction of the tensile sample was the direction of the provided rods. Since the microstructure was found to be isotropic, the sample orientation with respect to the tensile direction should not affect mechanical properties. Creep tests were performed using a lever type creep machine. In the present work, all the creep tests were carried out in air at a temperature of 480 °C. Applied stress was varied between 150 and 500 MPa. Elongation of the sample was measured by a differential transformer with an accuracy of ± 1.5 μm. Temperature was controlled by a thyristor regulator within ± 1 °C. Variation of creep strain and temperature was recorded at a time interval of 2 to 10 minutes by a data logger.

The crept samples were air-cooled to room temperature and the microstructure was observed by a transmission electron microscope (TEM). TEM samples were prepared by cutting a 3-mm disk, ground to approx. 100 μm, subsequently jet polished to form perforation using a solution of perchloric acid at approximately –30 °C.

3. RESULTS AND DISCUSSION

Fig. 4 shows creep curves of the Ti-6-22-22S tested at 480 °C under various stresses. Strain in the vertical axis is a plastic strain. The curves are obtained by interpolating the experimental data points that have an error range of the strain measurement of approximately ± 1.5 μm. The experimental data can be fitted well with a logarithmic equation of creep strain as a function of time. This is considered to be a normal creep behavior characterized by a logarithmic creep. Fig. 5 shows a relationship between stain and strain rate. In all cases, strain rate decreases gradually with increasing strain. Initial strain rate varies in the range of 10^{-6} to 10^{-7} s^{-1} as stress is varied from 150 to 500 MPa

Time to reach a creep strain of 0.1% at 480 °C is converted to Larson-Miller parameter given by $(T+255.6)(20+\log t)$. Here, T and t are, respectively, temperature in °C and time in hour to reach 0.1% creep strain. Figure 6 shows a Larson-Miller plot. The reported data of other titanium alloys are also included in the figure for comparison [10]. Dotted lines correspond to the (α+β) Ti alloys while solid lines correspond to the near-α Ti alloys. In all examined stress values, Larson-Miller parameter of Ti-6-22-22S is much larger than Ti-6Al-4V (Ti-64), indicating a better creep resistance. At stresses above 300 MPa, the creep resistance of Ti-6-22-22S is comparable to Ti-6Al-2Sn-4Zr-6Mo (Ti-6246) and is better than Ti-6Al-2Sn-4Zr-2Mo (Ti-6242). This result is in agreement with the previous reports by Bartlo et al. for 0.2% creep strain, as shown in Fig. 1. At stresses below 300 MPa, on the other hand, creep resistance of the alloy is still much better than Ti-64 but becomes worse than that of Ti-6242. (The data of Ti-6246 are not available for low stresses.) The datum point at the lowest stress of 150 MPa may be an indication that the slope of the curve becomes less steep and extends to

larger values of Larson-Miller parameter than expected from extrapolation of the thick dotted line. This trend is clearly seen in the case of Ti-8Al-1Mo-1V, Ti-5Al-2.5Sn, Ti-6Al-4V alloys.

Fig. 7 shows a TEM bright-field image of the samples crept to a strain of 0.1% at 150 MPa and 250 MPa. The images show dislocation substructure in an α lamellar . The images are obtained under a two-beam condition with a strong diffracted beam of $10\bar{1}1$. The electron beam direction was along $[1\bar{1}0\bar{1}]$. Under this condition, all types of dislocations in the hcp structure can be imaged. It is obvious that the dislocation density increases with increasing stress from 150 MPa to 250 MPa. Planar defects are also observed at 250 MPa. The trace of these planar defects are (0001) and $(01\bar{1}\bar{1})$ planes. These traces appears to be the traces of $\{1\bar{1}01\}$ twins or stacking faults. The formation of $\{1\bar{1}01\}$ twins have been investigated in detail under tensile deformation conditions in a wide temperature range [11-13]. Dissociation of sessile dislocation has also been observed and theoretically discussed [14, 15].

Fig. 8 shows a selected-area diffraction pattern of the α lamellar. Strong spots are indexed for the α phase, while weak spots are superlattice spots of the α_2 phase. The presence of the superlattice spots has been reported in various Ti alloys, and the precipitation of the α_2 phase has been suggested [16]. A clear evidence of α_2 precipitation has been reported only recently in a limited case in Ti-6-22-22S alloy after aging the alloy for the maximum time of 1000 hours [17]. Up to date, an equilibrium phase diagram of the Ti-Al binary system is available above 500 °C. According to the phase diagram at 500 °C, the Al concentration of 6 wt.% is considered to be in a single α phase region. Thus, α_2 precipitation would not be expected, despite the fact that the precipitation has been observed in many cases. In consistent with the experimental observation, recent computer simulation indicated that the phase boundary between α and $(\alpha+\alpha_2)$ lies on the Ti richer side than expected from the reported equilibrium phase diagram [18]. This tendency was found to become more prominent at temperatures below 500 °C. Therefore, it appears that re-evaluation of the equilibrium phase diagram is needed. Nonetheless, the precipitation of the α_2 phase increases the mechanical strength at elevated temperatures in a stronger extent than expected from a normal solution hardening mechanism

[19].

In the TEM images, precipitation of silicides are not observed. Evans et al. reported that the silicide of $Ti_xZr_{5-x}Si_3$ is formed by aging approximately above 700 °C. On the other hand, α_2 is stable below 705~735 °C. Wood et al. also reported that the silicides is not formed after the same triplex heat treatment as employed in the present work [6].

4. CONCLUSION

The $\alpha+\beta$ processed Ti-6-22-22S alloy was studied for its creep resistance at 480 °C under stresses of 150 to 500 MPa. Initial strain rate was in the range of 10^{-6} to 10^{-7} s^{-1}. Creep resistance was evaluated by Larson-Miller time for 0.1% plastic strain. The creep resistance of the investigated alloy was found to be similar to the Ti-6Al-2Sn-4Zr-6Mo (Ti-6246) alloy and to be much better than the Ti-6Al-4V alloy. Under the present experimental condition, dislocation glide appeared to be a major deformation mechanism.

Based on the present results, I conclude that the Ti-6-22-22S alloy can be used for creep-resistant applications at intermediate temperatures near 400 °C and lower. Together with excellent room-temperature mechanical properties in the previous reports by others, this alloy may replace the existing Ti-6246 alloy and can be used for a wide range of applications.

REFERENCES

1. S. R. Seagle, G. S. Hall, and H. B. Bomberger, Titanium Science and Technology, (TMS, Pittsburgh, 1973), p. 1981.
2. H. R. Phelps and J. R. Wood, Titanium í92 Science and Technology, (1992), p. 193
3. G. W. Kuhlman, K. A. Rohde, and A. K. Chakrabarti, Titanium í92 Science and Technology, (1992), p. 1371.
4. Lockheed Martin Aeronautical Systems, Advanced Materials and Processes, (1998), p. 23.
5. Lane Lineberger, ibid., p. 45.
6. J. R. Wood, T. J. Tomczyk, and H. R. Phelps, Titaniumí95: Science and Technology, Ed. P. A. Blenkinsop, W. J. Evans, and H. M. Flower, (Inst. Mater., The University Press, Cambridge, 1996), p. 1500.
7. P. Russo and R. Boyer, Materials Properties Handbook, Titanium Alloys, Ed. R. Boyer, G. Welsch, and E. W. Collings (ASM International, Materials Park, OH, 1994), p.719.
8. L. J. Bartlo, H. B. Bomberger, and S. R. Seagle, AFML-TR-73-122, Battele Columbus Lab (1973).
9. G. Wegmann, J. Arbrecht, G. Lutjering, K-D. Folkers, and C. Liesner, Z. Metallkd. 88, 764 (1997).
10. S. Lampman, Properties and Selection: Nonferrous Alloys and Special Purpose Materials, Vol. 2, ASM Handbook, ASM International, Materials Park, OH (1990), p. 592
11. N. E. Paton and W. E. Backofen, Metall. Trans. 1, 2839 (1970)
12. A. Akhtar, Metall. Trans. 6A, 1105 (1975)
13. S. Fujishiro and J. W. Edington, Tech. Report. AFML-TR-70-176 (1970).
14. M. Sob, Phys. Stat. Sol. (a), 24K, 133 (1974)
15. M. Sob, J. Kratochvil, and F. Kroupa, Czech J. Phys. B25, 872 (1975).
16. D. J. Evans, T. F. Broderick, J. B. Woodhouse, and J. R. Hoeningman, Titanium '95: Science and Technology, Ed. P. A. Blenkinsop, W. J. Evans, and H. M. Flower, (Inst. Mater., The University Press, Cambridge, 1996), p. 2413
17. X. D. Zhang, J. M. K. Wiezorek, W. A. Baeslack III, D. J. Evans, and H. L. Fraser, Acta mater. 46, 4485 (1998).
18. H. Liew, J. Koike, G. D. W. Smith, and A Cerezo, to be published (1998).
19. J. Koike, K. Egashira, and H. Oikawa, Mater. Sci. Eng. A213, 98 (1996).

FIGURES

Fig. 1 Larson-Miller plot for 0.2% plastic strain. Open circles are data for the β processed Ti-6-22-22S by Kuhlman et al. [3]. Filled circle are data for the α+β processed Ti-6-22-22S by Bartlo et al. [8].

Fig. 2 (a) Optic micrograph and (b) TEM bright-field image of the triplex heat treated alloy.

Fig. 3 The size of a tensile sample.

Fig. 4 Creep strain as a function of time at 480 °C for various stresses.

Fig. 5 Strain rate as a function of creep strain at 480 °C for various stresses.

Fig. 6 Larson-Miller plot for 0.1% plastic strain. Filled circled are the experimental data obtained in the present work.

Fig. 7 TEM bright-field images of the samples crept to a strain of 0.1% at σ=150 and at σ=250 MPa.

Fig. 8 Selected area diffraction pattern of the crept sample at 150 MPa to 0.1%.

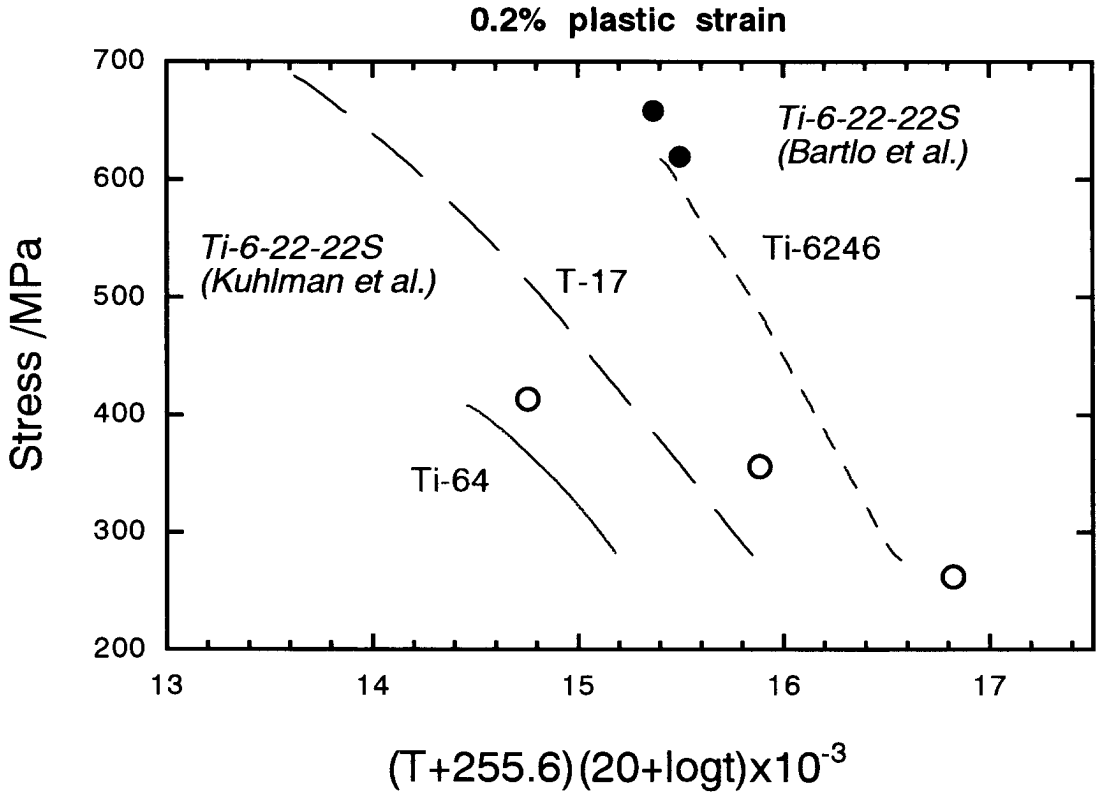
0.2% plastic strain
700
600
500
400
300
200
Stress /MPa
13
14
15
16
17
(T+255.6)(20+logt)x10-3
Ti-6-22-22S
(Bartlo et al.)
Ti-6246
Ti-6-22-22S
(Kuhlman et al.)
T-17
Ti-64

Fig. 1

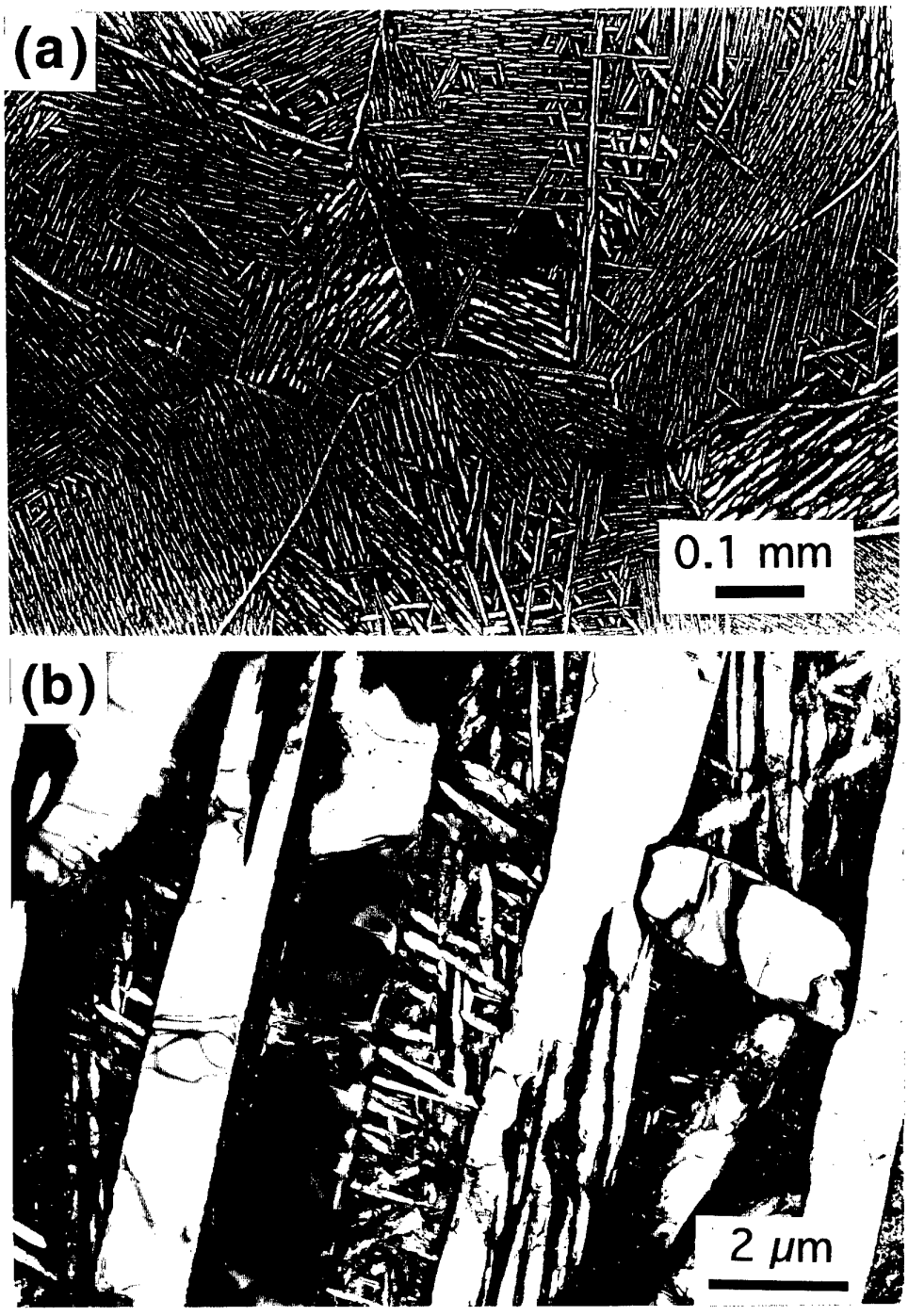

Fig. 2

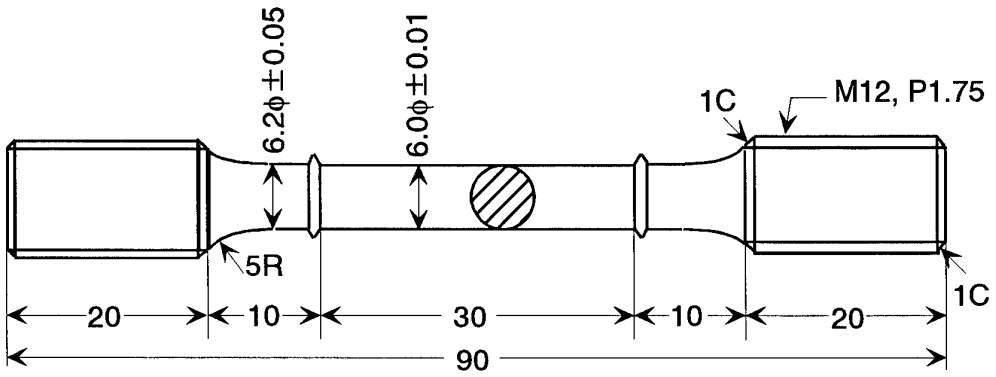

Fig. 3

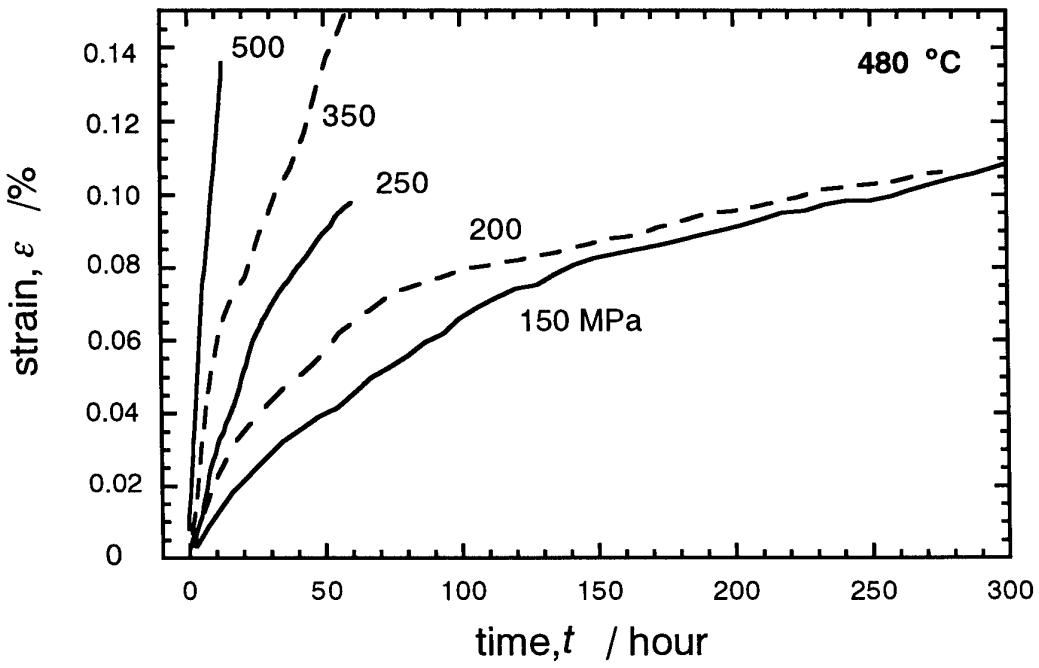
0.14
0.12
0.10
0.08
0.06
0.04
0.02
0
strain, ε /%
500
350
250
200
150 MPa
480 °C
0
50
100
150
200
250
300
time, t / hour

Fig. 4

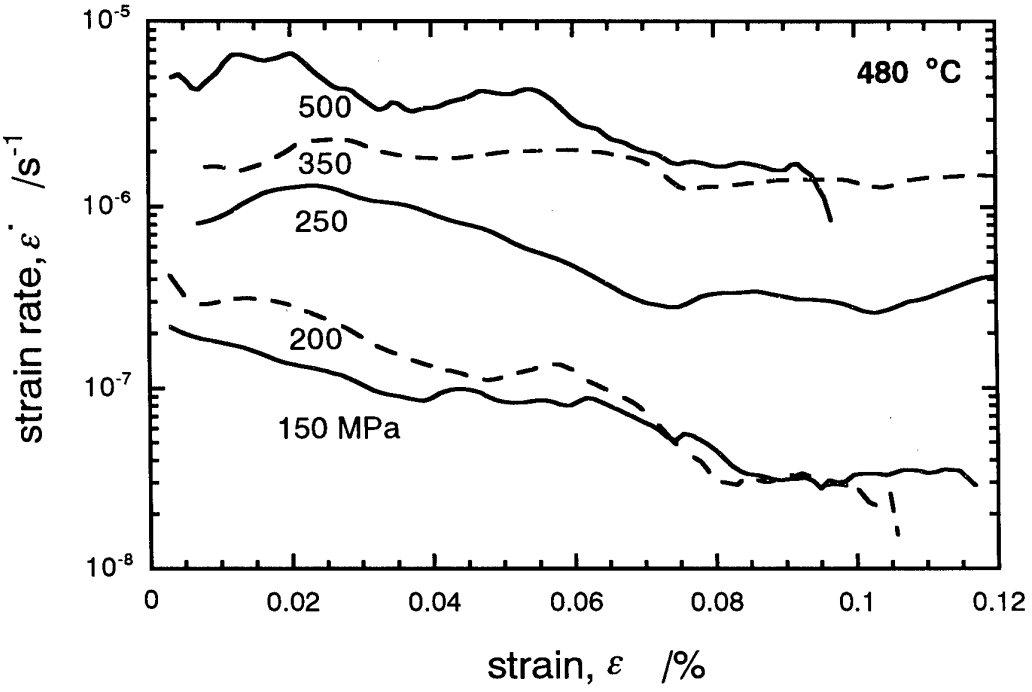
480 °C
500
350
250
200
150 MPa
strain rate, $\dot{\varepsilon}$ /s^{-1}
strain, ε /%
10^{-5}
10^{-6}
10^{-7}
10^{-8}
0
0.02
0.04
0.06
0.08
0.1
0.12

Fig. 5

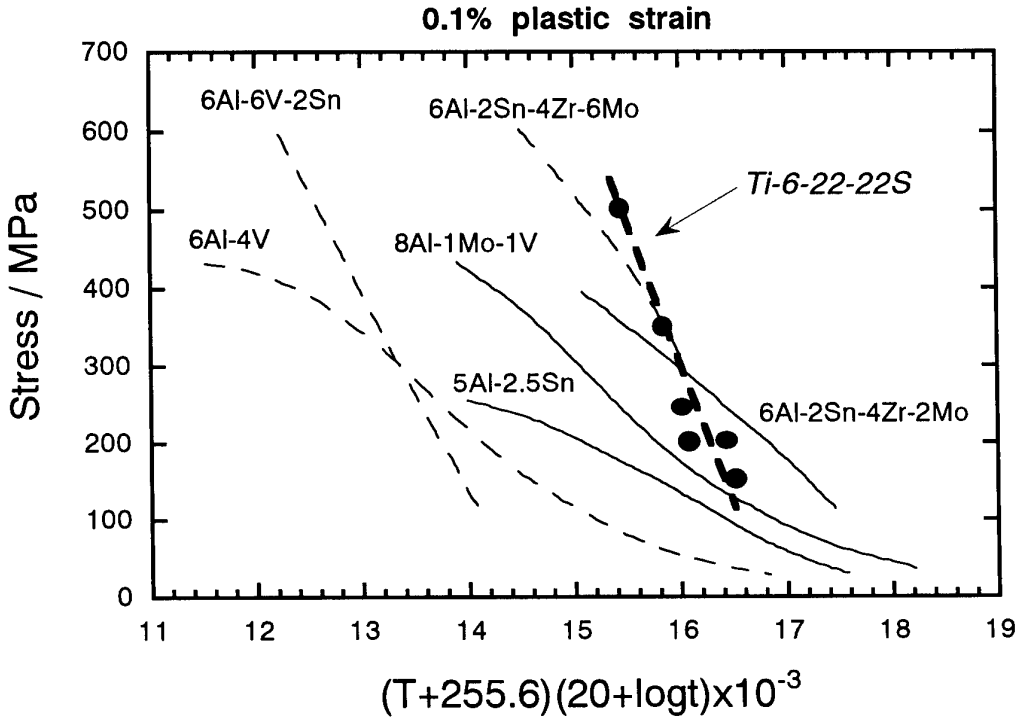
0.1% plastic strain
Stress / MPa
700
600
500
400
300
200
100
0
11
12
13
14
15
16
17
18
19
(T+255.6)(20+logt)x10-3
6Al-6V-2Sn
6Al-2Sn-4Zr-6Mo
Ti-6-22-22S
6Al-4V
8Al-1Mo-1V
5Al-2.5Sn
6Al-2Sn-4Zr-2Mo

Fig. 6

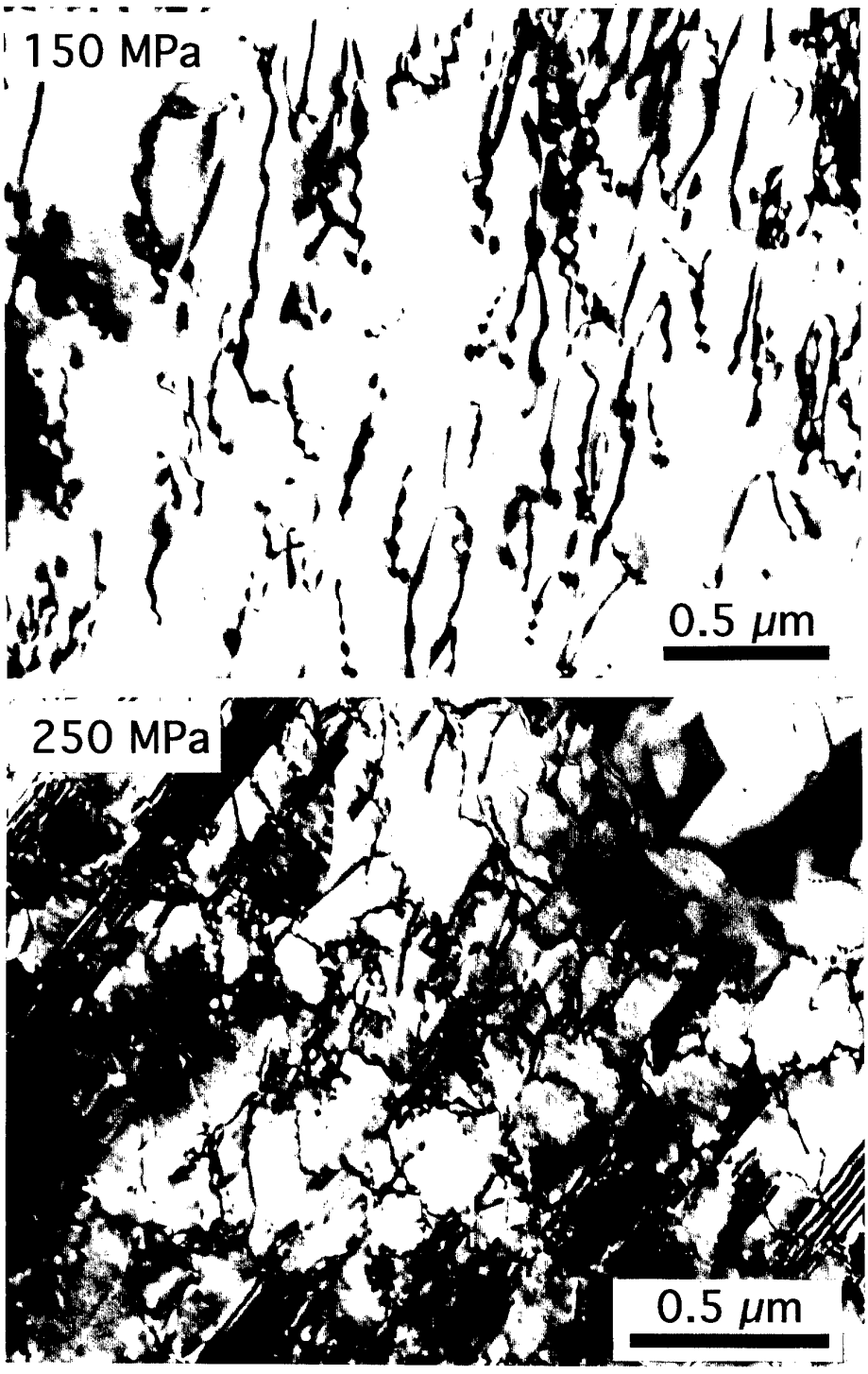

Fig. 7

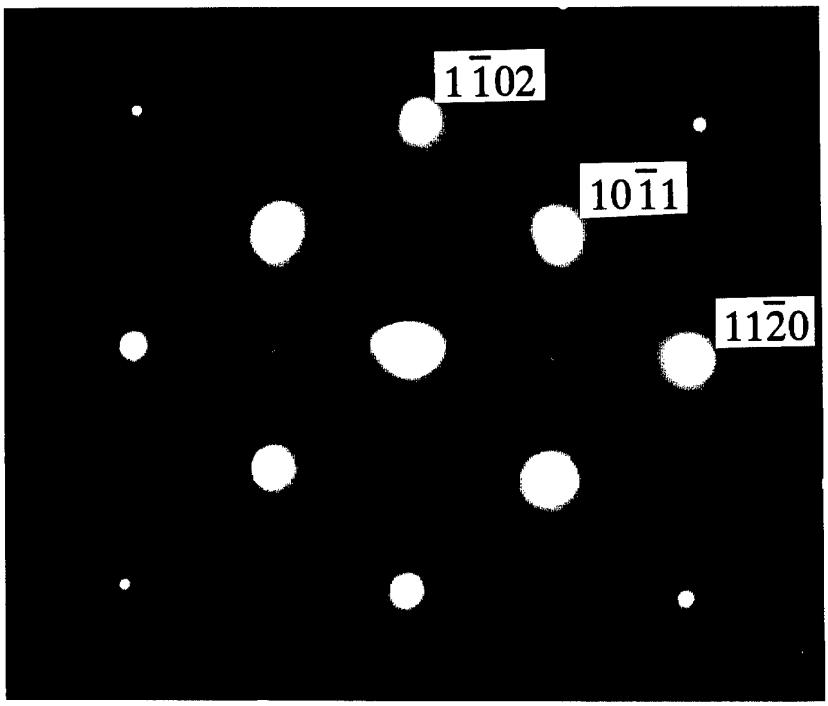

Fig. 8